Open Access Journal

Journal of Power Technologies 98 (1) (2018) 20–29

journal homepage:papers.itc.pw.edu.pl

Nanocrystallines as core materials for contactless power transfer (CPT)

Prabhat Chandra Ghosh[a,*], Pradip Kumar Sadhu[a], Ankita Ghosh[b], Nitai Pal[a]

[a] *Department of Electrical Engineering, Indian Institute of Technology (ISM), Dhanbad - 826004, India;*
[b] *Department of Electrical Engineering, PVG's College of Engineering and Technology, Pune - 411003, India*

Abstract

Efficient contactless power transfer (CPT) is an emerging technology which is attracting great scientific interest because it can mitigate some of the problems commonly associated with conventional wired power transfer systems. CPT systems suffer from very low efficiency because of the poor coupling coefficient, which is due to the large air gap between the transmitter and receiver coils. Therefore, CPT transformers are mostly operated at high frequencies to improve the quality factor of transmitter and receiver coils and thus counterbalance the effect of the low coupling coefficient. On the other hand, informed selection and design of core materials for CPT transformers can improve the coupling coefficient and thereby boost the overall power transfer efficiency of the system. However, at high power and high frequency CPT applications, core losses become very high and play an important role in determining the efficiency of the system. This paper reports on a detailed investigation into the suitability of nanocrystallines as core materials for high power and high frequency CPT systems.

Keywords: Contactless power transfer; mutual inductance; coupling coefficient; core materials; ferrites; nanocrytallines

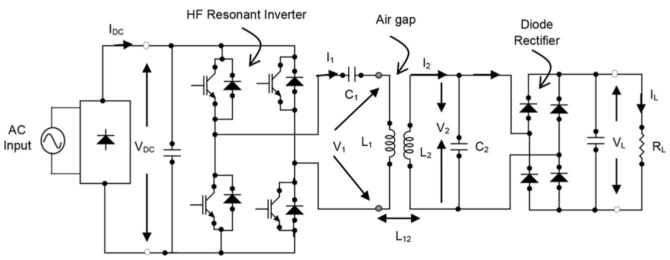

Figure 1: Circuit schematic of a contactless power transfer system

1. Introduction

Contactless power transfer (CPT) is achieved by mutual inductance between two coils through the air gap. However, in a conventional transformer the flux links between two coils through core materials, giving a high coefficient of magnetic coupling. In contactless power transfer, as the flux links between two coils through the air-gap, the coupling coefficient is very poor: 0.1 to 0.6 compared with over 0.95 in a conventional transformer. Therefore, the efficiency of the system is very poor [1]. Hence, when striving to meet the ever-increasing consumer demand for convenient portable CPT devices, there is huge scope for exploring the potentials of magnetic inductive contactless power transfer systems. The basic concepts of CPT technology as shown in Fig. 1 have been explained in detail in numerous papers [1–4]. However, inadequate discussion has been devoted to the subject of selecting suitable transformer core materials for contactless power transfer.

The magnetic material for transformer core design of CPT systems is a crucial issue. Due to the poor coupling coefficient in CPT systems, transformers are operated at high frequency to improve the quality factor of the system and hence overall efficiency. Soft magnetic materials are commonly used as the core materials of transformers and inductors due to their superior magnetic properties. Hence, the characteristics of soft magnetic materials have to be explored and then tradeoffs made according to the needs and specifications of the particular application. Ferromagnetic materials are adopted for high-power, high-frequency transformer core materials due to their higher saturation level compared to ferrites, but they are not suitable at very high frequency because of increased losses. Therefore, at high frequency ferrites are the only option, due to their high resistivity. Soft ferrites are commonly used as core materials for CPT transformers on account of their low loss characteristics and medium saturation level. Nanocrystalline materials, which are still somewhat of a novelty, have been are attracting great interest as high-frequency high-power core materials owing to their favorable magnetic and electrical proper-

*Corresponding author
Email address: pcghoshcme@gmail.com (Prabhat Chandra Ghosh)

ties. Therefore, they can be explored as suitable core materials for CPT systems.
The potential of nanocrystallines for the high frequency high power transformer core materials used for CPT systems needs detailed analysis. While high permeability and low coercivity of soft magnetic materials are required for transformer cores, low conductivity is also very important to reduce the eddy current losses since they operate under AC conditions. Particularly in high frequency CPT systems, eddy current loss plays an important role because of their low efficiency. In general, ferrites exhibit better loss performance at high frequency due to their high resistivity, but with lower saturation flux density. That is why efforts are ongoing to discover new core materials which have high resistivity and high saturation flux density. Nanocystalline materials seem to have solved all these problems. This paper goes on to discuss the characteristics of ferrites and then investigate and determine the suitability and superiority of nanocrystallines for CPT applications [5–7].

2. Mathematical modelling of a CPT system

The power output P_{out} of a CPT system is expressed by the open-circuit voltage V_{OC}, short-circuit current I_{SC} and the quality factor Q as shown in (1). This can also be written in terms of the VA at the input terminals of the primary circuit $V_1 I_1$, the transformer coupling coefficient k and the quality factor Q_2 of the secondary circuit [2–4].

$$P_{out} = P_{SU} Q_2 = V_{OC} I_{SC} Q_2 = \omega I_1^2 \frac{L_{12}^2}{L_2} Q_2 = V_1 I_1 k^2 Q_2 \quad (1)$$

where: P_{SU}—the uncompensated power rating.
P_{SU}, V_{OC} and I_{SC} are given by

$$P_{SU} = V_{OC} I_{SC}, \quad V_{OC} = j\omega L_{12} I_1, \quad I_{sc} = \frac{L_{12} I_1}{L_2}. \quad (2)$$

The angular frequency of the primary (transmitter) current I_1 is ω and V_1 is the voltage across L_1. The mutual inductance between primary (transmitter) and secondary (receiver) circuits is L_{12}. L_2 is the inductance of the secondary circuit under no load condition. The operational frequency and power rating of the CPT system are limited by the switching devices used. Both factors have to be balanced against switching losses and copper losses. An IGBT based full bridge resonant inverter has been considered. VA ratings, tolerances, and degradation of CPT systems over time, restrict the practical operational quality factor Q from 4 to 6 [8]. Coupling coefficient k is the ratio of the flux that links both primary and secondary coils to the total flux produced by the secondary coil.

Coupling coefficient k plays an important role in CPT system performance. The coupling coefficient of CPT systems is very low due to high leakage fluxes, as the air gap between the primary and secondary coils is large. The value of the coupling coefficient of a CPT system ranges from 0.15 to 0.6. It ensures the overall feasibility, cost effectiveness, and efficiency of the whole system. The coupling coefficient can be easily determined by measuring L_{12}, L_1 and L_2 with an LCR meter. Mutual inductance is highly dependent on the air gap distance between primary and secondary coils, whereas L_2 is determined by coil parameters such as size and number of turns in the coil [9–11].

Values of L_1 and L_2 do not depend on the position of primary and secondary coils. As discussed above, independent of their power level, CPT systems suffer from low magnetic coupling due to the high leakage inductance of the coils caused by the large air gap between the transmitter and the receiver coils. It imposes an inherent limitation on the efficiency of power transfer of CPT systems [10, 11].

The efficiency can be improved by resonant compensation of the receiver with either a parallel or a series connected compensation capacitor. This is shown in Fig. 1. Another series or parallel connected capacitor is added at the primary side in order to reduce the reactive power requirement from the source, thereby improving the overall efficiency of the system.

Therefore, if both sides of the resonant circuit are tuned to the same resonance frequency ω_0, the current in the transmitter coil is approximately sinusoidal.

Primary coil quality factor Q_1 and secondary coil quality factor Q_2 can be expressed as:

$$Q_1 = \frac{\omega_0 L_1}{R_1}, \quad Q_2 = \frac{\omega_0 L_2}{R_2}. \quad (3)$$

The inductor quality factor Q of the two coils is the geometric average of the two individual coil quality factors [9] and is given by:

$$Q = \sqrt{Q_1 Q_2} \quad (4)$$

It can be shown that for both compensation topologies (series or parallel) on the secondary side, the maximum power transfer efficiency η_{max} of the CPT system is expressed as [9–11]:

$$\eta_{max} = \frac{(kQ)^2}{\left(1 + \sqrt{1 + (kQ)^2}\right)^2} \quad (5)$$

where: k—magnetic coupling between primary and secondary coils.

Equation (5) shows that maximum power transfer efficiency η_{max} depends on the figure of merit (FOM), where FOM= kQ. For high values of the FOM, in (5) η_{max} is approximated as:

$$\eta_{max} \approx 1 - \frac{2}{(kQ)} \quad (6)$$

In (6), η_{max} is the maximum efficiency, which depends on the winding's quality factor Q and the coupling coefficient k if the core loss is neglected. In (1), it is clear that if ω and I_1 are constant, designs of L_{12} and L_1 ensure the overall feasibility, cost effectiveness, and efficiency of the complete CPT

Table 1: Typical properties of Ferrites at 25°C [5]

Grade/Category	B_{sat}, T	μ_i	ρ, $\Omega - m$	T_c, °C	Thermal conductivity, W/mK
3F3 (MnZn)	0.45	2000	2	220	3.5~5
3C94 (MnZn)	0.45	2300	5	220	3.5~5
3F45 (MnZn)	0.5	900	10	300	3.5~5
4B1 (NiZn)	0.35	250	10^5	250	3.5~5
4F1 (NiZn)	0.35	80	10^5	260	3.5~5

system. L_{12} is highly dependent on air gap distance and misalignment between transmitter and receiver coils, whereas L_2 is determined by the coil parameters such as size and number of turns in the coil. Due to the inherently large air gaps in CPT system, L_2's position relative to L_1 does have some small effect on both inductances.

The coupling coefficient can also be improved by suitable selection of core materials. At high frequency, core loss cannot be ignored for certain core materials. However, core loss at high frequency can be minimized by informed selection of core materials. Therefore, to maximize the power transfer efficiency (PTE) of CPT systems, the FOM of CPT systems should be as high as possible. On the other hand, the FOM can be enhanced by the right selection of core materials. This paper explores the suitability of core materials for high frequency CPT systems and it establishes that nanocrystallines are the right choice as core materials for CPT systems [12].

3. Soft ferrites as high frequency core materials

Yogoro Kato and Takeshi Takei of the Tokyo Institute of Technology invented ferrite in 1930. Since 1950, ferrite materials have been developed for high-frequency applications because of their high electrical resistivity and low eddy current losses. The spectrum of applications of ferrites in electronic circuitry continues to grow. The wide range of possible geometries, the continuing improvements in the material characteristics and their relative cost-effectiveness make ferrite components the default choice for both conventional and innovative applications [5]. A ferrite is a type of ceramic compound composed of iron oxide (Fe_2O_3) combined chemically with one or more additional metallic elements (i.e. Zinc, Nickel, Manganese and Copper) [6, 13–15]. Metal oxides are added in various amounts to create many different materials whose properties can be modified for a variety of applications. Ferrite components are pressed from a powdered precursor and then sintered (fired) in a furnace. The mechanical and electromagnetic properties of the ferrite are heavily affected by the sintering process, which is time-temperature-atmosphere dependent [12–17]. The typical properties of MnZn and NiZn ferrites, according to data from Ferrox-cube (previously Philips), are listed in Table 1.

Ferrites are ferromagnetic materials and are electrically nonconductive, being ceramic in nature. Combinations of few substances exhibit these two properties. Ferrites can

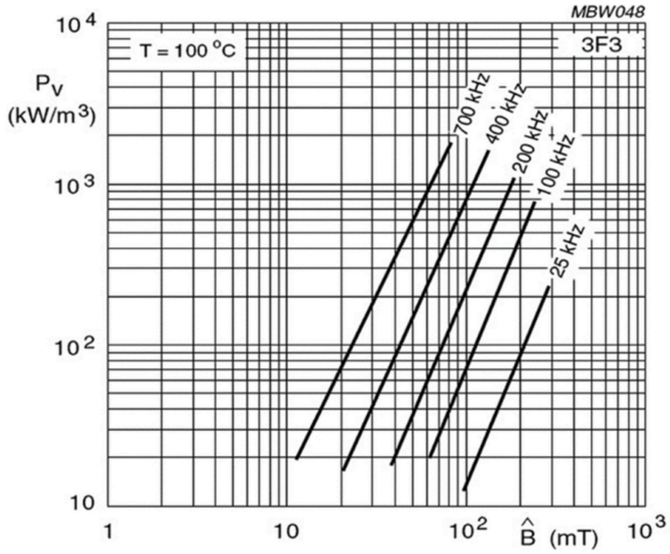

Figure 2: Ferrite 3F3 core loss density at 25°C [5]

be classified into two families based on their magnetic coercivity. Hard ferrites have high coercivity; it is difficult to magnetize or demagnetize them. They are used to make permanent magnets, for use in devices such as refrigerator magnets, loudspeakers and small electric motors. Soft ferrites, having low coercivity, can be easily magnetized or demagnetized. Soft ferrites with high resistivity prevent eddy current losses [5, 6, 9, 16, 17]. Due to their comparatively low losses at high frequencies, they are extensively used in the cores of high frequency transformers and inductor applications such as switched-mode power supplies, contactless power supply etc. The saturation flux density of ferrites is between 0.3~0.5 Tesla normally and permeability varies from thousands to several tens of thousands.

Typically, NiZn ferrites have lower saturation flux density and better loss performance at high frequency, compared to the MnZn ferrites. Therefore, NiZn ferrites are preferred for ultra-high frequency applications. As the operating frequency increases, the core loss density of ferrites will increase as shown in Fig. 2, and consequently permeability will reduce as shown in Fig. 3. The above two effects are very important and must be considered when designing transformer cores for CPT systems where magnetic coupling is a major concern, because both of them could lead to a design failure in the transformer.

The operating temperature of ferrites should be below the Curie temperature, at which magnetic material suddenly loses magnetic characteristics. Normally, the maximum continuous operating temperature of ferrites is below 125°C. The development of high temperature ferrite (up to 300°C) is a new area of research and has attracted great interest [16–21]. Within the specified temperature range the main drawback of ferrite is temperature dependency, which is a major concern when selecting core materials for contactless power transfer. Fig. 4 shows the saturation flux density, initial permeability and core-loss-density variations of ferrite 3F3 un-

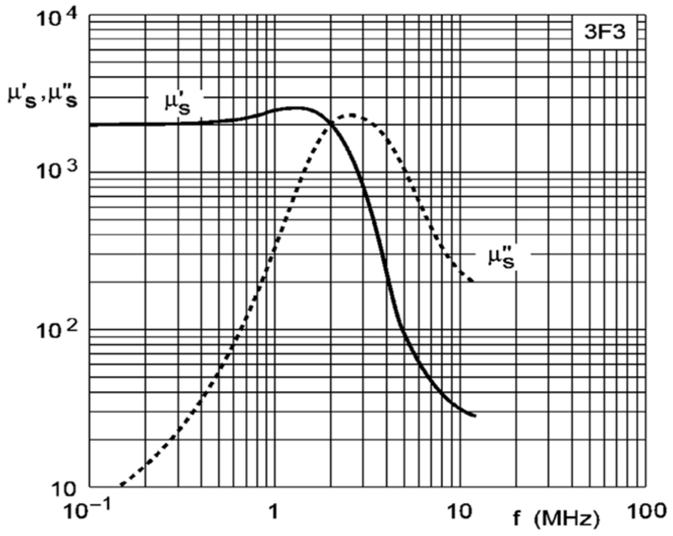

Figure 3: Ferrite 3F3 complex permeability as a function of frequency [5]

Table 2: Typical properties of nanocrystalline ($Fe_{73.5}Cu_1Nb_3Si_{15.5}B_7$) at 100 kHz

Grade/Category	B_{sat}, T	μ_i	$\rho, \Omega - m$	T_c, °C	Density, gms/cm^3
Nanocrystalline	1.23	11×10^4	1.15×10^{-6}	600	7.24–7.3

Table 3: Simulation parameters

Parameter	Value
Transformer turns ratio	11:11
Transmitter coil inner / outer diameter, cm	10 / 35.5
Receiver coil inner / outer diameter, cm	10 / 35.5
Transmitter core dimension, cm	38×38×0.5
Receiver core dimension, cm	38×38×0.5
Transmitter aluminum shield dimension, cm	40×40×0.5
Receiver aluminum shield dimension, cm	40×40×0.5
Air gap, cm	12
Misalignment, cm	2.5

der various temperatures [5]. It shows that saturation flux density decreases as the operating temperature increases. Accordingly, it imposes a major design constraint when designing cores for high-frequency-high-power CPT systems for a particular application. The reduction in permeability with increases in operating temperature will result in variations in circuit inductance. In turn, variations in inductance will affect the resonance of the circuit, thereby increasing the reactive power demand. The most important concern at this point is the variation in loss with the temperature. All of the above mentioned temperature dependent issues of ferrites impact the feasibility of ferrites for high-frequency-high-power CPT applications. Therefore, ferrite core based high power high frequency CPT systems require special cooling arrangements and hence there are limitations on the use of ferrite core in CPT systems.

4. Choice of nanocrystallines as core materials for CPT systems

The name itself defines the nature of the material. By definition, a nanocrystalline is a polycrystalline material with a crystallite size of only a few nanometers. These materials fill the gap between amorphous materials without any long-range order and conventional coarse-grained ferromagnetic (CRGO steel) materials. Nanocrystalline has a crystallite grain size below 100 nm. Grain sizes from 100–500 nm are typically considered “ultrafine” grains. Changes in grain size change magnetic properties to a great extent. In 1988, Yoshizawa and others invented a new class of iron-based alloys named nanocrystallines [21]. It is observed that nanocrystallines exhibit superior soft magnetic properties better than supermalloys.

The observed properties were outstanding, and unique for high frequency core building. The magnetic characteristics of nanocrystalline materials are given in Table 2. Nanocrystallines have a raft of suitable properties like lower losses, higher permeability and near zero magnetostriction compared to all previously-known soft magnetic materials as shown in Fig. 5. These all-favorable properties of nanocrystallines make them ideally suited for high frequency high power applications like CPT systems and other high frequency power electronics devices [23, 24]. Also these properties make the product smaller in size and lighter in weight, which are very desirable aspects in light of the much sought-after portability of the system for marketing purposes. In conventional ferromagnetic materials, coercivity increases as the grain size decreases, which is totally contrary to soft magnetic materials. Diametrically opposed results are observed in the case of nanocrystallines. An extremely fine grained structure leads to good magnetic properties in nanocrystallines, as illustrated in Fig. 6 [22, 25]. Thus nanocrystallines fill the gap between amorphous and crystalline materials [26–30]. CPT systems have to be operated at high frequency due to poor magnetic coupling. So, core materials play a crucial role in their design. On the other hand, at high operating frequency, thermal behavior of core materials also changes.

Table 4: Simulation results with / without core and shielding

CPT system	Mutual inductance, mH	Coupling coefficient
CPT Transformer without core and shield	0.665	0.214
CPT Transformer with ferrite core	1.973	0.326
CPT Transformer with nanocrystalline core	2.21	0.388
CPT Transformer with ferrite core and shielding	1.911	0.298
CPT Transformer with nanocrystalline core and shielding	2.01	0.331

Table 5: Coupling coefficients using nanocrystalline core and aluminum shield for variable air gap and misalignment

Misalignment, cm	Cpl coef (coil 1, coil 2) Air gap = 4.5 cm	Cpl coef (coil 1, coil 2) Air gap = 9 cm	Cpl coef (coil 1, coil 2) Air gap = 13.5 cm	Cpl coef (coil 1, coil 2) Air gap = 18 cm	Cpl coef (coil 1, coil 2) Air gap = 22.5 cm
0	0.769288	0.479345	0.288368	0.177059	0.112392
3	0.728367	0.458072	0.278054	0.171540	0.109372
6	0.615321	0.399417	0.248453	0.156049	0.101310
9	0.456459	0.315134	0.204659	0.133126	0.088677
12	0.285872	0.220968	0.154015	0.105587	0.073053
15	0.134826	0.130902	0.103551	0.077282	0.056787

5. Analysis of a CPT system with and without core materials

The effectiveness of nanocrystallines for contactless power transfer (CPT) has been validated by finite element analysis (FEA) of the CPT transformer using a 3-D finite element tool (Maxwell). The results were compared with ferrite cores as well. Simulation parameters are given in Table 3. From the simulation results given in Table 4, it is observed that the coupling coefficient is very much affected by the core materials. A two-coil CPT system without core material at an air gap of 12 cm and misalignment of 2.5 cm is shown in Fig. 7a. Its flux density distribution is shown in Fig. 7b. It is obvious from the flux density distribution in Fig. 7b that leakage flux is very high thereby reducing the mutual inductance and coupling coefficient as shown in Table 4. The mutual inductance and coupling coefficient of the CPT system without using core material are merely 0.665 mH and 0.214 respectively. Whereas, using ferrite cores as shown in Fig. 8a, leakage flux has been reduced significantly. Therefore, mutual inductance and coupling coefficient have been increased to 1.973 mH and 0.326 respectively as given in Table 4. Flux density distribution with ferrite core has been shown in Fig. 8b. In Fig. 8c, it is observed that with using nanocrystalline core there is further improvement in mutual inductance and flux density under the same operating conditions and they are increased to 2.21 mH and 0.388 respectively. Moreover, by adding the aluminum shield as shown in Fig. 9a and Table 4 mutual inductance and the coupling coefficient were reduced due to the shielding effect. Their flux density distributions are given in Fig. 9b and 9c respectively.

Therefore, it is clear that the mutual inductance / coupling coefficient can be improved sufficiently using carefully selected core material. From the above results, it is clear that replacing ferrite cores with nanocrystalline cores does little to improve the mutual inductance / coupling coefficient of the system. Changes in the coupling coefficients by using nanocrystalline core and aluminum shield for variable air gap and misalignment are shown in Table 5 and Fig. 10 respectively. It is observed from Table 5 that a small increase in misalignment at a particular air gap causes a significant decrease in the coupling coefficient.

Misalignment is a common phenomenon in a CPT system. Therefore, some amount of misalignment should always be factored in when modelling a CPT system for variable air gap. It can been seen from Table 5 and Fig. 10 that maximum coupling coefficient is attained when the center of the transmitter coil is aligned to the center of the receiver coil. So, maximum efficiency of the CPT system can be achieved at this position.

Nevertheless, during application, some amount of misalignment always occurs in the system. For example, at an air gap of 4.5 cm without misalignment, the coupling coefficient is 0.769. However, at the air gap of 4.5 cm with misalignment of 3 cm, the coupling coefficient falls to 0.728 as shown in Table 5. During design of a CPT system for any particular application, close consideration must be given to the effect of misalignment as it is a common concern of a movable charging system.

6. Loss performance of nanocrystalline core materials

The eddy current effect on ferrite and nanocrstalline cores was also analyzed at 20 kHz frequency using 3-D finite element tool (Maxwell). It can be seen in Fig. 11a and Fig. 11b that the eddy current effect is more prominent in ferrite core than in nanocrystalline core because of the higher electrical resistivity of nanocrystalline core. Hysteresis loss density (W/m^3) is also greater in ferrite core than in nanocrystalline core, as is shown in Fig. 11c and 11d respectively. Therefore, nanocrystalline cores are more energy efficient than ferrite cores. At high frequency and high power applications, the use of nanocrystalline cores in place of ferrite cores can improve the efficiency of CPT systems to some extent. However, ferrites currently enjoy the lion's share of the market for high frequency core materials due to their easy availability and universality.

From all of the above results, it is evident that nanocrystalline core material is the best choice for high frequency and high power applications, because of its all-favorable magnetic and electrical properties. Due to its high saturation flux density and high electrical resistivity, it provides enhanced efficiency for systems in high-frequency-high-power applications.

7. Conclusions

Core materials for high-frequency-high power transformers of CPT systems need rigorous investigation. In this paper, a suitable core material is sought for high frequency and high power CPT systems, which suffer from low efficiency. Therefore, a search was undertaken to identify a core material of low losses, high operating temperature, zero magnetotriction and high permeability, which remains constant at high frequencies. After intensive investigation nanocrystalline core material was found to be the ideal candidate as the core material for CPT systems, which operate at high frequency and have the properties of high Curie temperature, high initial linear permeability, near zero magnetotriction, high electrical resistivity and good thermal conductivity. This paper has explored all possible and suitable high frequency core materials and finally has selected nanocrystalline core materials as the best choice for CPT systems.

The major benefits of this class of high-tech materials are: (i) miniaturization of the system in volume, (ii) high degree of universality in shape, and (iii) superb magnetic and electrical properties. This opens the way for a reduction in size for the whole CPT system, since transformer core materials account for a large proportion of the weight and volume and cannot be replaced with conventional soft magnetic materials. With technological advances, demand for CPT systems is rising sharply. Therefore, the price of the product is becoming competitive compared to conventional crystalline materials. In sum, nanocrystalline core materials can mitigate some of the key issues surrounding the efficiency of CPT systems.

References

[1] D. A. Pedder, A. D. Brown, J. A. Skinner, A contactless electrical energy transmission system, IEEE Transactions on Industrial Electronics 46 (1) (1999) 23–30.

[2] J. Boys, G. Covic, A. W. Green, Stability and control of inductively coupled power transfer systems, IEE Proceedings-Electric Power Applications 147 (1) (2000) 37–43.

[3] J. Hou, Q. Chen, S.-C. Wong, K. T. Chi, X. Ruan, Analysis and control of series/series-parallel compensated resonant converter for contactless power transfer, IEEE Journal of Emerging and Selected Topics in Power Electronics 3 (1) (2015) 124–136.

[4] R. Bosshard, J. W. Kolar, Inductive power transfer for electric vehicle charging: Technical challenges and tradeoffs, IEEE Power Electronics Magazine 3 (3) (2016) 22–30.

[5] Data sheets soft ferrite products and accessories.
URL `http://www.ferroxcube.com`

[6] G. Herzer, Amorphous and nanocrystalline soft magnets, Kluwer Academic Publishers, 1997.

[7] R. Kolano, A. Kolano-Burian, K. Krykowski, J. Hetmańczyk, M. Hreczka, M. Polak, J. Szynowski, Amorphous soft magnetic core for the stator of the high-speed pmbldc motor with half-open slots, IEEE Transactions on Magnetics 52 (6) (2016) 1–5.

[8] W. Zhong, S. Hui, Maximum energy efficiency tracking for wireless power transfer systems, IEEE Transactions on Power Electronics 30 (7) (2015) 4025–4034.

[9] L. Yuan, B. Li, Y. Zhang, F. He, K. Chen, Z. Zhao, Maximum efficiency point tracking of the wireless power transfer system for the battery charging in electric vehicles, in: Electrical Machines and Systems (ICEMS), 2015 18th International Conference on, IEEE, 2015, pp. 1101–1107.

[10] P. Sergeant, A. Van den Bossche, Inductive coupler for contactless power transmission, IET Electric Power Applications 2 (1) (2008) 1–7.

[11] J. Zhang, X. Yuan, C. Wang, Y. He, Comparative analysis of two-coil and three-coil structures for wireless power transfer, IEEE Transactions on Power Electronics 32 (1) (2017) 341–352.

[12] S. Zurek, Fem simulation of effect of non-uniform air gap on apparent permeability of cut cores, IEEE Transactions on Magnetics 48 (4) (2012) 1520–1523.

[13] X. Xin, D. R. Jackson, J. Chen, Wireless power transfer along oil pipe using ferrite materials, IEEE Transactions on Magnetics 53 (3) (2017) 1–5.

[14] I.-G. Lee, N. Kim, I.-K. Cho, I.-P. Hong, Design of a patterned soft magnetic structure to reduce magnetic flux leakage of magnetic induction wireless power transfer systems, IEEE Transactions on Electromagnetic Compatibility 59 (6) (2017) 1856–1863.

[15] C. A. Stergiou, V. Zaspalis, Impact of ferrite shield properties on the low-power inductive power transfer, IEEE Transactions on Magnetics 52 (8) (2016) 1–9.

[16] L. Li, Y. Fang, Y. Liu, Preparation and application on antenna of soft ferrite core for wireless sensor networks, IEEE Transactions on Magnetics 51 (11) (2015) 1–3.

[17] W. Ding, X. Wang, Magnetically coupled resonant using mn-zn ferrite for wireless power transfer, in: Electronic Packaging Technology (ICEPT), 2014 15th International Conference on, IEEE, 2014, pp. 1561–1564.

[18] Y. Han, G. Cheung, A. Li, C. R. Sullivan, D. J. Perreault, Evaluation of magnetic materials for very high frequency power applications, IEEE Transactions on Power Electronics 27 (1) (2012) 425–435.

[19] A. J. Hanson, J. A. Belk, S. Lim, C. R. Sullivan, D. J. Perreault, Measurements and performance factor comparisons of magnetic materials at high frequency, IEEE Transactions on Power Electronics 31 (11) (2016) 7909–7925.

[20] R. Prochazka, J. Hlavacek, K. Draxler, Magnetic circuit of a high-voltage transformer up to 10 khz, IEEE Transactions on Magnetics 51 (1) (2015) 1–4.

[21] X. Liu, Y. Wang, M. R. Islam, G. Lei, C. Liu, J. Zhu, Comparison of electromagnetic performances of amorphous and nanocrystalline core-based high frequency transformers, in: Electrical Machines and Systems (ICEMS), 2014 17th International Conference on, IEEE, 2014, pp. 2028–2032.

[22] J. Petzold, Advantages of softmagnetic nanocrystalline materials for modern electronic applications, Journal of Magnetism and Magnetic Materials 242 (2002) 84–89.

[23] S. Purushotham, R. Ramanujan, Thermoresponsive magnetic composite nanomaterials for multimodal cancer therapy, Acta biomaterialia 6 (2) (2010) 502–510.

[24] K. Pan, Y. Dong, W. Zhou, G. Wang, Q. Pan, Y. Yuan, X. Miao, G. Tian, Tio2-b nanobelt/anatase tio2 nanoparticle heterophase nanostructure fabricated by layer-by-layer assembly for high-efficiency dye-sensitized solar cells, Electrochimica Acta 88 (2013) 263–269.

[25] T. Kauder, K. Hameyer, Performance factor comparison of nanocrystalline, amorphous, and crystalline soft magnetic materials for medium-frequency applications, IEEE Transactions on Magnetics 53 (11) (2017) 1–4.

[26] Y. Liu, Y. Han, F. Lin, L. Li, Performance evaluation of fe-based nanocrystalline cores with high and low residual flux, IEEE transactions on plasma science 42 (8) (2014) 2079–2085.

[27] W. Shen, F. Wang, D. Boroyevich, C. W. Tipton IV, High-density nanocrystalline core transformer for high-power high-frequency resonant converter, IEEE Transactions on Industry Applications 44 (1) (2008) 213–222.

[28] Hitachi, Power electronics component catalog Finemet F3CC series cut core (April 2016).

[29] F. D. Tan, J. L. Vollin, S. M. Cuk, A practical approach for magnetic core-loss characterization, IEEE Transactions on Power Electronics 10 (2) (1995) 124–130.

[30] C. Cuellar, A. Benabou, N. Idir, High frequency model of ferrite and nanocrystalline ring core inductors, in: Power Electronics and Applications (EPE'15 ECCE-Europe), 2015 17th European Conference on, IEEE, 2015, pp. 1–8.

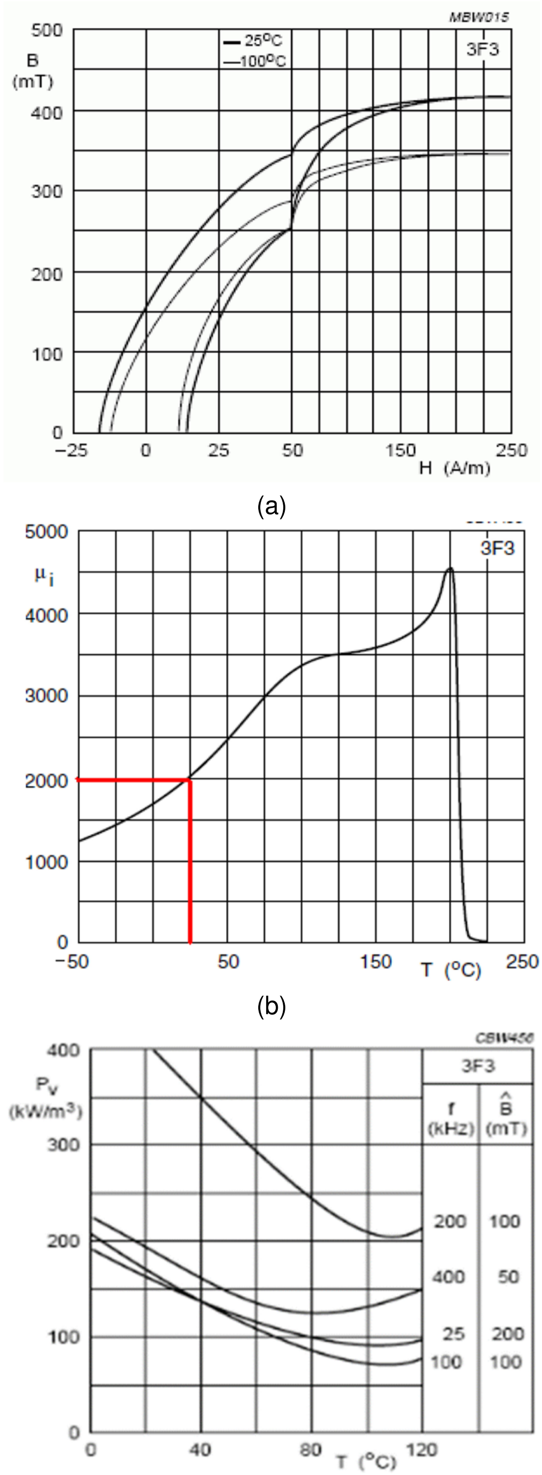

Figure 4: Typical characteristics of ferrite 3F3 as a function of temperature: (a) B-H curve, (b) Initial permeability, (c) Core loss density [5]

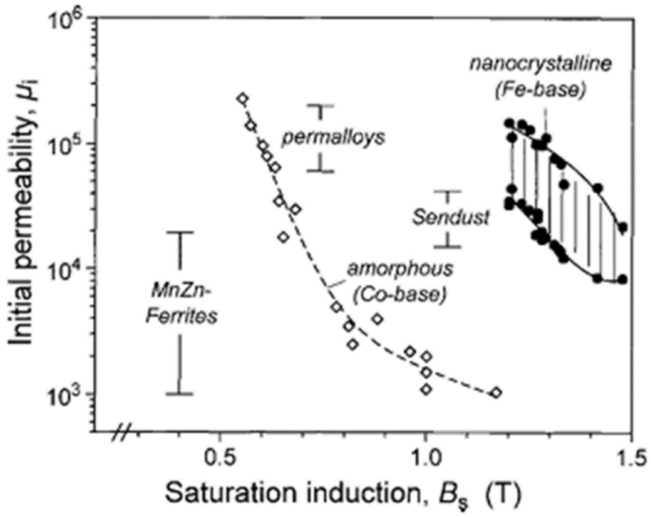

Figure 5: Typical initial permeability and saturation flux density for different soft magnetic materials [6]

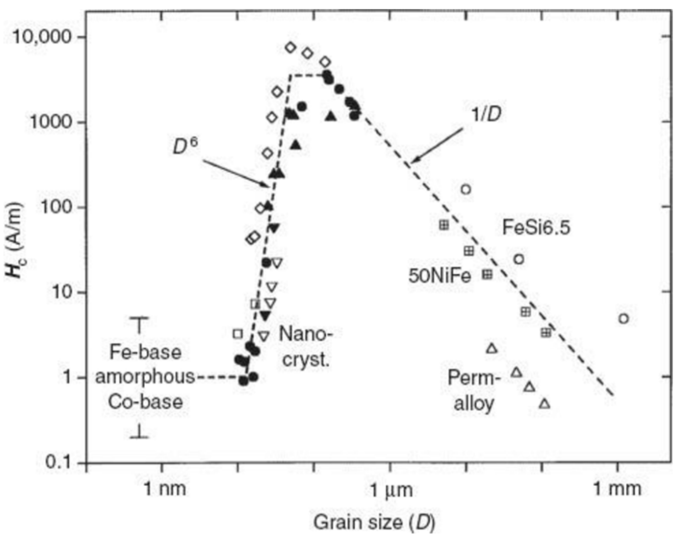

Figure 6: The relation between coercivity and grain size of various ferro-magnetic materials [22]

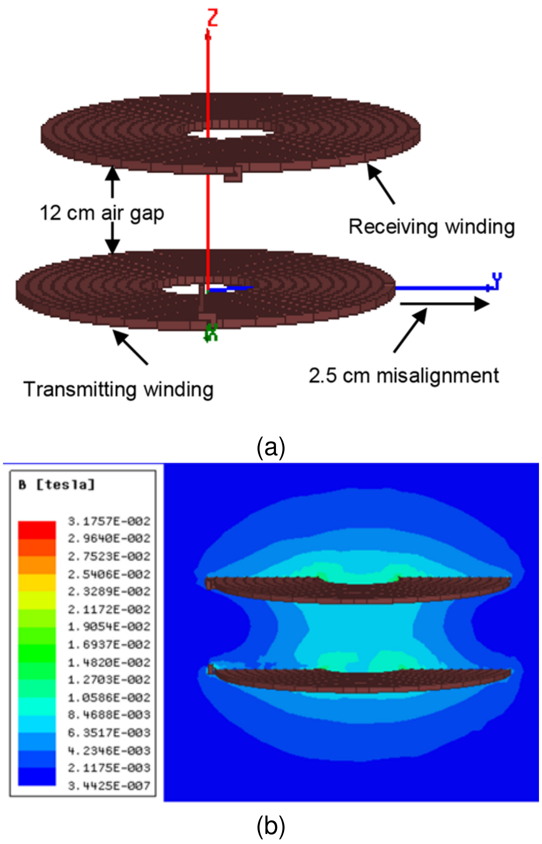

Figure 7: Two-coil CPT system without core: (a) Simulation schematic, (b) Flux density distribution

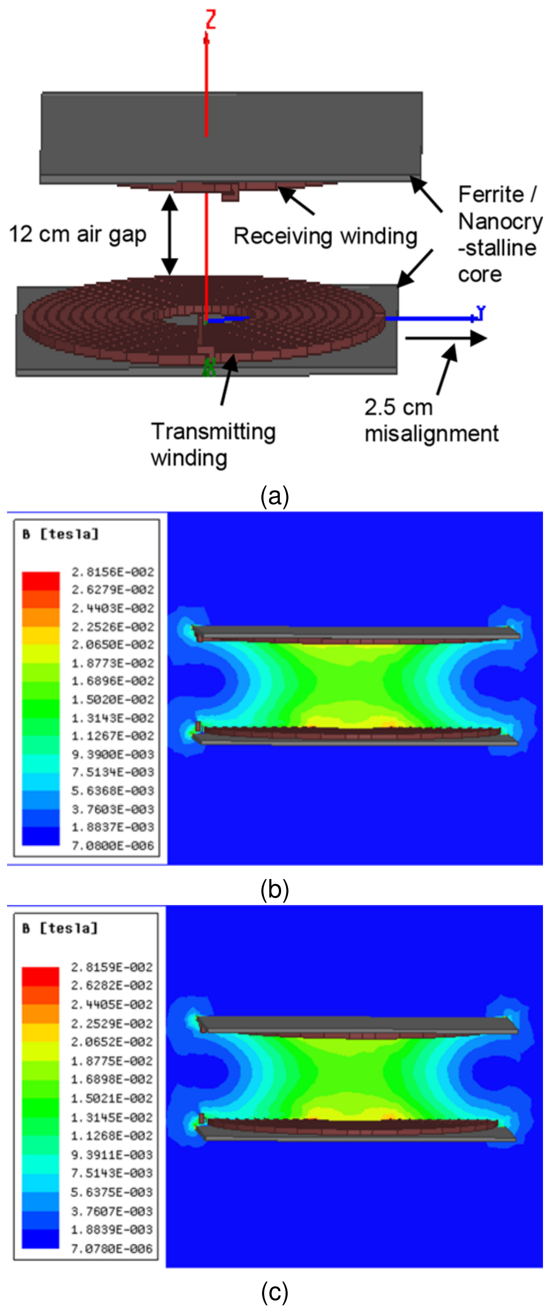

Figure 8: Two-coil CPT system with core: (a) Simulation schematic with ferrite / nanocrytalline core, (b) Flux density distribution with ferrite core, (c) Flux density distribution with nanocrystalline core

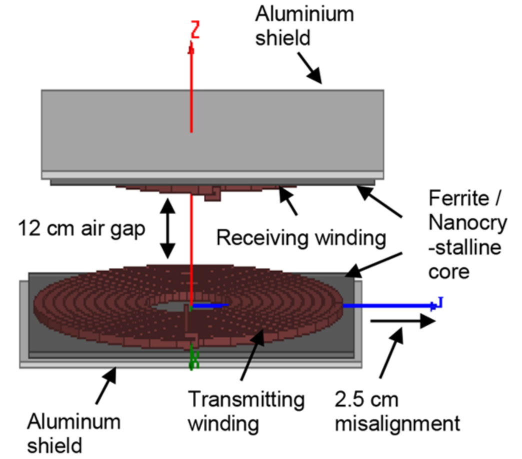

(a)

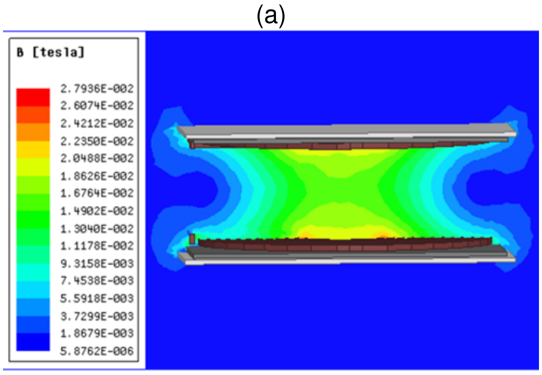

(b)

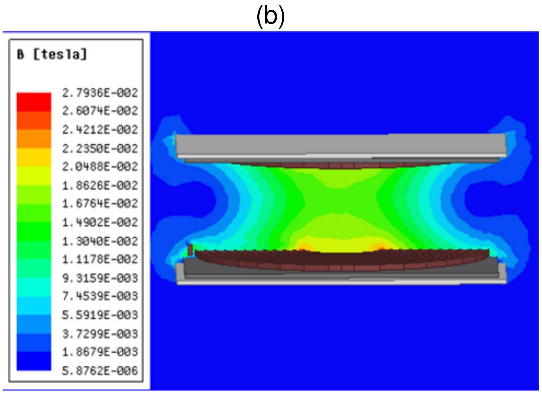

(c)

Figure 9: Two-coil CPT system with core and shield: (a) Simulation schematic with ferrite / nanocrystalline core and aluminum shield, (b) Flux density distribution with ferrite core and aluminum shield, (c) Flux density distribution with nanocrystalline core and aluminum shield

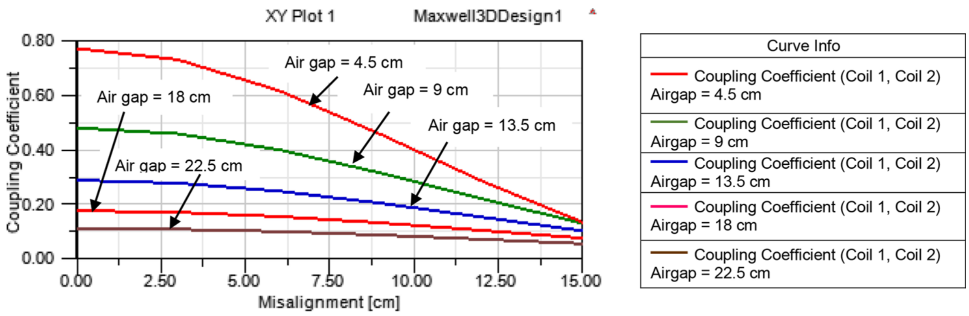

Figure 10: Coupling coefficients using nanocrystallline core and aluminum shield at variable air gap and misalignment

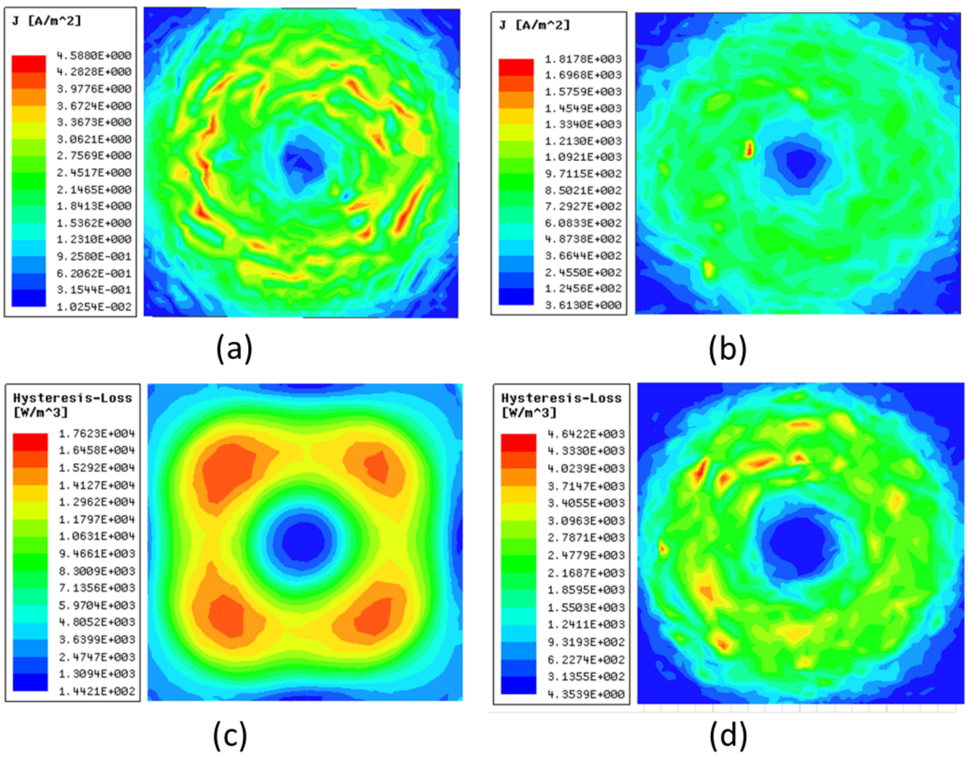

Figure 11: Eddy current effect and hysteresis loss density on core materials at 20 kHz frequency: (a) Eddy current effect on ferrite core, (b) Eddy current effect on nanocrystalline core, (c) Hysteresis loss density on ferrite core, (d) Hysteresis loss density on nanocrystalline core